see commentary on page 253

In vivo regulation of the heme oxygenase-1 gene in humanized transgenic mice

Junghyun Kim[1,2,7], Abolfazl Zarjou[2,3,7], Amie M. Traylor[2,3], Subhashini Bolisetty[2,3], Edgar A. Jaimes[2,3], Travis D. Hull[4], James F. George[4], Fady M. Mikhail[5] and Anupam Agarwal[2,3,6]

[1]Department of Pathology, University of Alabama at Birmingham, Birmingham, Alabama, USA; [2]Department of Medicine, University of Alabama at Birmingham, Birmingham, Alabama, USA; [3]Nephrology Research and Training Center, University of Alabama at Birmingham, Birmingham, Alabama, USA; [4]Department of Surgery, University of Alabama at Birmingham, Birmingham, Alabama, USA; [5]Department of Genetics, University of Alabama at Birmingham, Birmingham, Alabama, USA and [6]Department of Veterans Affairs Medical Center, Birmingham, Alabama, USA

Heme oxygenase-1 (HO-1) catalyzes the rate-limiting step in heme degradation, producing equimolar amounts of carbon monoxide, iron, and biliverdin. Induction of HO-1 is a beneficial response to tissue injury in diverse animal models of diseases including acute kidney injury. *In vitro* analysis has shown that the human *HO-1* gene is transcriptionally regulated by changes in chromatin conformation, but whether such control occurs *in vivo* is not known. To enable such an analysis, we generated transgenic mice, harboring an 87-kb bacterial artificial chromosome expressing human HO-1 mRNA and protein and bred these mice with HO-1 knockout mice to generate humanized BAC transgenic mice. This successfully rescued the phenotype of the knockout mice including reduced birth rates, tissue iron overload, splenomegaly, anemia, leukocytosis, dendritic cell abnormalities, and survival after acute kidney injury induced by rhabdomyolysis or cisplatin nephrotoxicity. Transcription factors such as USF1/2, JunB, Sp1, and CTCF were found to associate with regulatory regions of the human *HO-1* gene in the kidney following rhabdomyolysis. Chromosome conformation capture and ChIP-loop assays confirmed this in the formation of chromatin looping *in vivo*. Thus, these bacterial artificial chromosome humanized HO-1 mice are a valuable model to study the human *HO-1* gene, providing insight to the *in vivo* architecture of the gene in acute kidney injury and other diseases.

Kidney International (2012) **82,** 278–291; doi:10.1038/ki.2012.102; published online 11 April 2012

KEYWORDS: acute renal failure; gene transcription; heme oxygenase

Correspondence: *Anupam Agarwal, Division of Nephrology, THT 647, University of Alabama at Birmingham, 1900 University Boulevard, Birmingham, Alabama 35294, USA. E-mail: agarwal@uab.edu*

[7]These authors contributed equally to this work.

Received 31 March 2011; revised 23 December 2011; accepted 17 January 2012; published online 11 April 2012

Heme oxygenase (HO) is an enzyme that catalyzes the initial and rate-limiting reaction in heme catabolism, resulting in the production of carbon monoxide, iron, and biliverdin.[1–3] Two isoforms of heme oxygenase have been characterized: an inducible enzyme, HO-1, and a constitutive isoform, HO-2. A third catalytically inactive isoform, HO-3, has been described but is suggested to be a pseudogene.[4] Besides its function in heme degradation and iron reutilization,[5,6] HO-1 exhibits potent cytoprotective effects via anti-inflammatory, anti-apoptotic, and anti-oxidant properties of its reaction products.[6,7] Because of the beneficial roles of HO-1 in various disease states including renal injury from ischemia–reperfusion injury,[8,9] glomerulonephritis,[10,11] nephrotoxins,[12] renal transplant rejection,[13–15] and rhabdomyolysis,[16,17] a large number of studies have explored the mechanisms of HO-1 transcription, translation, and its multiple functions using *in vitro* and *in vivo* model systems. Among them, a global HO-1 knockout mouse ($HO\text{-}1^{-/-}$) has been used widely as a model for studying the functions of HO-1 *in vivo*.[5,18] $HO\text{-}1^{-/-}$ mice show several phenotypical alterations including reduced live birth rates, tissue iron deposition, splenomegaly, increased sensitivity to oxidative stress and acute kidney injury, anemia, and leukocytosis.[5,18]

There have been studies using mouse models overexpressing HO-1 generated with cDNA constructs.[19–25] Organ-specific HO-1-overexpressing mice were generated to study the protective functions of HO-1 in cardiac diseases,[22] and global HO-1-overexpressing rats have also been characterized.[23] Gene delivery via viral vectors to transfer the *HO-1* gene has been tested in animal models.[26] However, despite the fact that the main function of HO-1, heme degradation and cytoprotection, is the same in both humans and rodents, it is difficult to utilize these models for mechanistic analysis of the human *HO-1* gene because of major differences between the molecular regulation of the mouse and human *HO-1* genes.[27] For instance, the human *HO-1* gene contains a potential cadmium response element, which has been identified at −4.0 kb of the 5′ flanking region of the *HO-1* gene.[28,29] However, the cadmium response element in the

mouse *HO-1* gene is immediately 3′ to this region, and is a nuclear factor (erythroid-derived 2)–like 2 sequence.[30] Heat shock and cytokines such as interferon-γ and hypoxia are potent inducers of HO-1 in rodent cells, but repress HO-1 expression in human cells.[28,31,32] Moreover, a 220-bp intronic enhancer that we recently identified in the human *HO-1* gene[33,34] is not present in the mouse *HO-1* gene. Therefore, generating a relevant *in vivo* model is a fundamental prerequisite to study human HO-1 regulation and expression.

We have shown that multiple regulatory regions within the *HO-1* gene interact with each other via chromatin looping and a transcription factor, specificity protein 1 (Sp1), mediates changes in chromatin conformation and initiation of human HO-1 transcription in renal epithelial cells *in vitro*.[33] Both positive and negative regulatory sequences in the human HO-1 promoter that bind to specific transcription factors have been described to control *HO-1* gene transcription *in vitro*. For example, JunB and upstream stimulatory factors 1 and (USF1/2) activate *HO-1* gene expression, whereas JunD acts as a repressor.[35,36] In order to investigate these findings including changes in chromosome conformation and associated transcription factors *in vivo*, an animal model of the human *HO-1* gene along with critical regulatory regions was developed. HO-1 bacterial artificial chromosome (BAC) mice were used to generate 'humanized' HO-1 (hHO-1) BAC mice containing the human *HO-1* gene but not the mouse *HO-1* gene and studied in rhabdomyolysis and cisplatin models of acute kidney injury *in vivo*.

RESULTS

Generation of HO-1 BAC transgenic mice

HO-1 BAC transgenic mice were generated by microinjection of purified BAC DNA containing the human *HO-1* gene (GenBank accession number: Z82244) depicted in Figure 1a into C57BL/6 oocytes. Two founders were obtained and genotyped by PCR using four primer pairs that amplify different regions within the BAC DNA (Table 1). As shown in Figure 1b, both founders carried the transgene and the copy number of the transgene was estimated by Taqman real-time PCR as described in the Materials and Methods. Estimated copy number of the two founders was 3 to 6. However, after the third generation (F3), copy number of all transgenic mice was between 1 and 2. Southern blot analysis on tail genomic DNA digested with *Eco*RI and probed with a 320-bp fragment within the *HO-1* gene revealed a single band at 8 kb (Figure 1c). Fluorescence *in situ* hybridization (FISH) analysis using HO-1 BAC as a probe showed a single integration site in peripheral blood (Figure 1d, right panel) and bone marrow cells (Figure 1e). Sequential metaphase FISH analysis localized the site of integration into chromosome 5 band qF (Figure 1e).

Characterization of HO-1 BAC transgenic mice

Monitoring body weight (Figure 2a) and blood pressure (data not shown) in the HO-1 BAC transgenic mice showed no significant differences compared with HO-1$^{+/+}$ mice. Furthermore, no difference in terms of growth, development, and survival were noted between HO-1 BAC compared with HO-1$^{+/+}$ mice. Tissues from HO-1 BAC transgenic and HO-1$^{+/+}$ mice were tested for HO-1 mRNA and protein expression. HO-1 mRNA levels were significantly higher (15–40-fold) in the heart, lung, liver, spleen, and kidney of the HO-1 BAC transgenic mice compared with the HO-1$^{+/+}$ tissues (Figure 2b). HO enzyme activity in tissues from HO-1 BAC mice was also increased compared with HO-1$^{+/+}$ mice (Figure 2c). In addition, HO-1 protein was overexpressed (2–3-fold higher) in aorta, brain, heart, lung, liver, spleen, intestine, skin, and kidney of HO-1 BAC transgenic mice compared with tissues from HO-1$^{+/+}$ mice (Figure 2d). HO-2 levels in the HO-1 BAC mice were similar to HO-1$^{+/+}$ mice (Figure 2d). These results indicate that HO-1 mRNA and protein are globally overexpressed in HO-1 BAC transgenic mice in the basal state and associated with increased HO enzyme activity, indicating that the over-expressed HO-1 protein in HO-1 BAC transgenic mice was functionally active.

To examine the localization of HO-1 expression in HO-1 BAC transgenic mice, immunohistochemistry was performed (Figure 2e). As expected, higher levels of HO-1 expression were observed in tissues (brain, heart, lung, liver, spleen, and kidney) of HO-1 BAC transgenic mice compared with HO-1$^{+/+}$ mice. The expected high basal HO-1 expression in the spleen was even higher in the HO-1 BAC transgenic mice. The staining pattern in the kidney showed the presence of HO-1 predominantly in renal proximal tubules, which was confirmed by colocalization with lotus lectin (Figure 2f).

Generation and characterization of humanized HO-1 BAC transgenic mice

Although the HO-1 BAC mice showed global overexpression of HO-1, the endogenous mouse *HO-1* gene is still intact in these mice. To overcome this limitation, HO-1 BAC mice were bred with HO-1$^{-/-}$ mice. Because of low number of live births from female HO-1$^{-/-}$ mice, we initially crossed female HO-1 BAC mice with male HO-1$^{-/-}$ mice to obtain HO-1$^{+/-}$ mice, which would carry the human HO-1 BAC transgene (BAC positive and HO-1$^{+/-}$). Then, these HO-1$^{+/-}$ BAC-positive mice were crossed with each other to obtain HO-1$^{-/-}$ mice expressing only the human *HO-1* gene (BAC positive and HO-1$^{-/-}$). The initial hHO-1 BAC transgenic mice were genotyped by using two primers that were used for genotyping HO-1 BAC transgenic mice (primers a and b, Table 1) and mouse HO-1 primers to confirm that the transgenic mice are indeed both BAC positive and mouse HO-1 negative (Figure 3a). Among five transgenic mice, three were HO-1 BAC positive (hHO-1 BAC 101, 104, and 105) and three were mouse-specific HO-1$^{-/-}$ for the mouse gene (hHO-1 BAC 103, 104, and 105). Thus, hHO-1 BAC 104 and 105 were determined to be both mouse-specific HO-1$^{-/-}$ and HO-1 BAC positive and referred to as hHO-1 BAC.

Using species-specific primers as listed in Table 1, further generations were genotyped to confirm the presence of

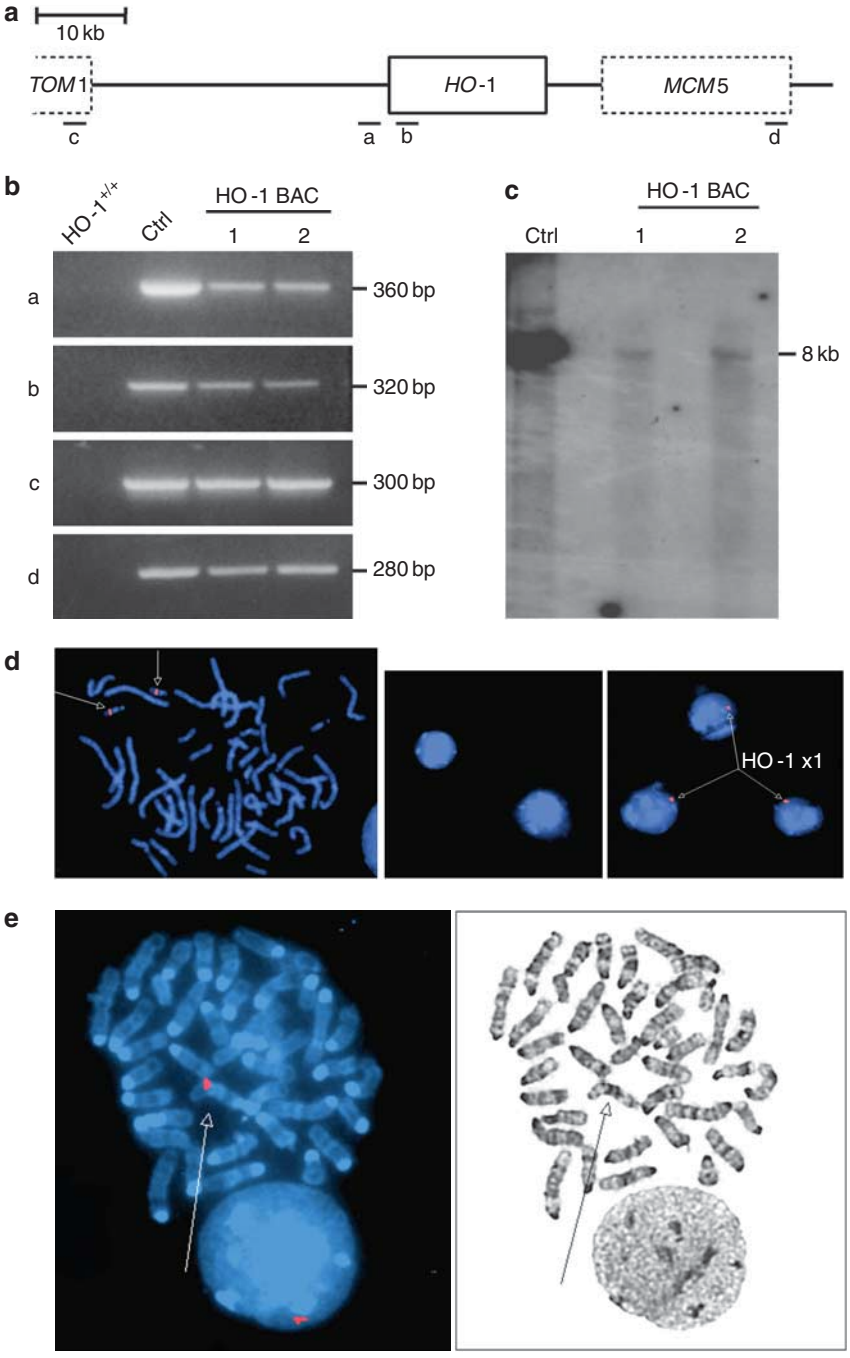

Figure 1 | Generation of heme oxygenase-1 (HO-1) bacterial artificial chromosome (BAC) transgenic mice. (**a**) Schematic of ~87 kb human BAC DNA (GenBank accession number: Z82244), a portion of human chromosome 22, containing the *HO-1* gene along with the 3′ end of *TOM1*, and *MCM5* genes used for the generation of HO-1 BAC mice is shown. a, b, c, and d represent the amplicons that were used to genotype the HO-1 BAC transgenic mice. Sequences of primers are listed in Table 1. (**b**) Four primer pairs were used to amplify regions a–d by PCR for genotyping the HO-1 BAC transgenic mice using tail DNA. DNA from wild-type C57BL6/J was used as a negative control (HO-1$^{+/+}$). Positive control was purified HO-1 BAC DNA used for the generation of HO-1 BAC transgenic mice. (**c**) Founder mice were identified by Southern blot analysis of tail DNA using a 320-bp PCR amplicon (region b) used as a probe after *Eco*RI digestion. Purified BAC DNA was used as a positive control (+Ctrl) and two founders (1 and 2) are shown. (**d**) Fluorescence *in situ* hybridization (FISH) analyses were performed on interphase peripheral blood cells from HO-1 BAC mice using the HO-1 BAC containing DNA as a probe (right panel). Human metaphase peripheral blood cells were used as positive control and arrows indicate the hybridization location of the HO-1 probe labeled in SpectrumOrange on chromosome 22 band q12.3 (left panel). Negative control using the HO-1 probe on peripheral blood cells from nontransgenic mouse (middle panel). (**e**) FISH analysis on HO-1 BAC transgenic bone marrow metaphase spread using the HO-1 BAC as a FISH probe labeled in SpectrumOrange (left panel). Note the single site of integration of the HO-1 BAC into chromosome 5 band qF (right panel).

Table 1 | Primers for genotyping, 3C, ChIP-loop, and ChIP assays

Assay	Name	Primer sequence (5′–3′)
Genotyping	BAC a For	GCCTCTGGGCTGTAGTGG
	BAC a Rev	AGTCGAGGTGGGAAGATTGCTT
	BAC b For	CATCTATGTGGCCCTGGAGGA
	BAC b Rev	CCAGGGCTTTCTGGGCAAT
	BAC c For	GCAGACCCAAGCGGGTAAG
	BAC c Rev	CCACTTCCCTGTCTGCACATTTC
	BAC d For	GGAACAACAGTTGATGCTCTGCTTCC
	BAC d Rev	CGGGACCCTGTGATTGATTGCTC
Characterization of hHO-1 BAC mice	Human-specific HO-1 For	CATGACACCAAGGACCAGAG
	Human-specific HO-1 Rev	AGTGTAAGGACCCATCGGAG
	Mouse-specific HO-1 For	GGTGATGGCTTCCTTGTACC
	Mouse-specific HO-1 Rev	AGTGAGGCCCATACCAGAAG
3C and ChIP-loop	F1	CTTGGGCTTGTCTTCCTTGCTGAAGAA
	F2	GAAAGCAAGCCCAGACCGGCAGC
	R1	CCCTTGGGAAACAAAGTCTGGCCATA
	R2	GCTAGTGAGGGACAGATGCCACCAAG
	Internal control For	GCTAATAGAGGCTGCACGATGTTTGGA
	Internal control Rev	GCCTAATATCACACAGCTCACCCGG
ChIP	220 bp enhancer For	ACAAGGCTGCATCTTAAAGC
	220 bp enhancer Rev	TCTCTGCCTGGGTGTGCACC
	−4.5 kb For	ATATGACTGCTCCTCTCCACCC

Abbreviations: 3C, chromosome conformation capture; BAC, bacterial artificial chromosome; ChIP, chromatin immunoprecipitation; For, forward; hHO-1 BAC, humanized HO-1 BAC; HO, heme-oxygenase; Rev, reverse.

human and absence of mouse HO-1 in hHO-1 BAC mice (Figure 3b). Next, the basal level of HO-1 protein expression in HO-1$^{+/+}$, HO-1$^{-/-}$, and hHO-1 BAC mice were examined in microsomal fractions from the kidney and spleen (Figure 3c). As illustrated, HO-1 protein expression was significantly higher in both the kidney and spleen of hHO-1 BAC mice compared with HO-1$^{+/+}$ mice and, as expected, no HO-1 expression was detected in the HO-1$^{-/-}$ samples. No significant differences were noted between HO-1 and HO-2 protein levels in the liver, lung, kidney, and spleen isolated from the HO-1 BAC and hHO-1 BAC (Supplementary Figure S1 online).

Human HO-1 in hHO-1 BAC transgenic mice rescues the phenotype of HO-1$^{-/-}$ mice

As hHO-1 BAC transgenic mice express human HO-1 in the HO-1$^{-/-}$ mice background, it is important to determine if the integrated human *HO-1* gene could rescue the phenotype of HO-1$^{-/-}$ mice. The fertility and live birth rate was notably increased when we crossed hHO-1 BAC mice compared with HO-1$^{-/-}$ breeding pairs from which no litters were obtained from at least 10 to 12 breeding pairs. Spleens from age-matched HO-1$^{+/+}$, HO-1$^{-/-}$, and hHO-1 BAC transgenic mice were compared (Figure 4a and b). All HO-1$^{-/-}$ mice had enlarged spleens with average length of 2.3 ± 0.4 cm. On the contrary, spleens from hHO-1 BAC mice were within the same range of length as the HO-1$^{+/+}$ mice (1.3 ± 0.2 and 1.2 ± 0.3 cm, respectively). Splenic weights were significantly higher in HO-1$^{-/-}$ mice, but this was also reversed in hHO-1 BAC mice (Figure 4b).

Decreased hemoglobin levels, leukocytosis, and reticulocytosis noted in HO-1$^{-/-}$ mice were reversed in hHO-1 BAC mice, and were similar to HO-1$^{+/+}$ mice (Figure 4c). Additionally, the hHO-1 BAC hematocrit was restored to normal levels (HO-1$^{+/+}$: 44 ± 0.7%, HO-1$^{-/-}$: 32.5 ± 2.5%, and hHO-1 BAC: 41 ± 0.5%, $P<0.05$ for HO-1$^{+/+}$ and hHO-1 BAC vs. HO-1$^{-/-}$). Kidneys of HO-1$^{-/-}$ mice showed increased iron deposition as previously described,[5,37] whereas iron was barely detected in tissues from HO-1$^{+/+}$ and hHO-1 BAC transgenic mice (Figure 4d). When compared with peripheral smears of HO-1$^{+/+}$ mice, HO-1$^{-/-}$ mice showed hypochromic microcytic anemia with considerable anisocytosis and fragmented red blood cells (RBCs; Figure 4e). However, the smears of hHO-1 BAC transgenic mice showed near-normal restoration of RBC morphology. Interestingly, RBCs from HO-1$^{-/-}$ and hHO-1 BAC mice displayed inclusions that mimicked Howell–Jolly bodies. These were also detected in peripheral smears of HO-1 BAC transgenic mice. The number of these inclusions in the peripheral smears of hHO-1 BAC mice was 1.54 per 100 RBCs compared with 0.1% in HO-1$^{+/+}$ mice and 0.4% in HO-1$^{-/-}$ mice.

We have recently reported that the proportion of splenic CD8^{+} dendritic cells (DCs) was significantly decreased in HO-1$^{-/-}$ mice.[38] To determine whether the human *HO-1* gene product in hHO-1 BAC mice could alter this phenotype, flow cytometry analysis of splenocytes from HO-1$^{+/+}$, HO-1$^{-/-}$, and hHO-1 BAC mice was performed. CD8^{+} DCs in HO-1$^{-/-}$ mice were significantly decreased compared with HO-1$^{+/+}$ mice, but splenocytes in hHO-1 BAC mice showed similar levels as HO-1$^{+/+}$ mice (Figure 4f and g).

Induction of rhabdomyolysis and cisplatin-induced kidney injury in hHO-1 BAC transgenic mice

To examine the response of HO-1$^{+/+}$ and hHO-1 BAC transgenic mice in heme-mediated renal injury, a model of

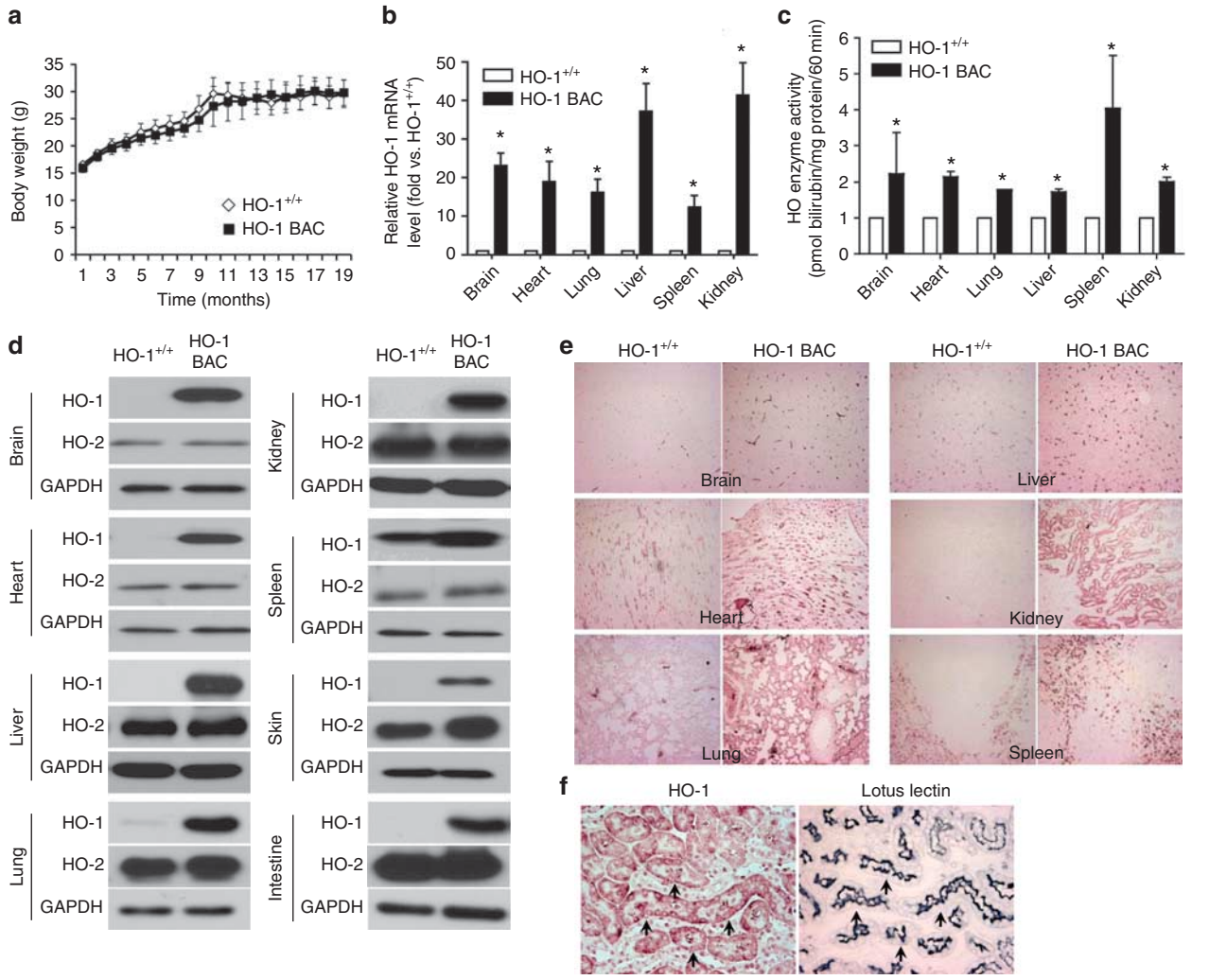

Figure 2 | Heme oxygenase-1 (HO-1) protein and mRNA are overexpressed in the organs of HO-1 bacterial artificial chromosome (BAC) transgenic mice. (**a**) Average body weights of HO-1 BAC mice ($n = 5$, solid square) and HO-1$^{+/+}$ mice ($n = 4$, open diamond) that were monitored for 19 months. (**b**) Total RNA was isolated from indicated organs and HO-1 mRNA expression level was quantified using real-time PCR. Glyceraldehyde 3-phosphate dehydrogenase (GAPDH) was used to normalize HO-1 mRNA levels. Results are shown as fold increase versus HO-1$^{+/+}$ from three independent experiments performed in triplicate each time (mean ± s.e.m.). *$P < 0.01$. (**c**) HO enzyme activity in the indicated organs of HO-1$^{+/+}$ and HO-1 BAC transgenic mice was compared. Results are shown as fold increase versus HO-1$^{+/+}$ from three independent experiments performed (mean ± s.e.m.). *$P < 0.05$. (**d**) Indicated tissues were harvested and HO-1 protein expression was determined by western analysis. Anti-GAPDH antibody was used as a loading control. (**e**) HO-1 expression was determined by immunohistochemistry using HO-1 antibody (SPA-896, Stressgen) in the brain, heart, lung, liver, spleen, and kidney tissues from HO-1$^{+/+}$ and HO-1 BAC transgenic mice. (**f**) Localization of HO-1 protein was determined by staining with lotus lectin (proximal tubule marker) and HO-1 on serial sections of kidneys from HO-1 BAC transgenic mice. Arrows indicate colocalization of HO-1 and lotus lectin in proximal tubules.

glycerol-induced rhabdomyolysis was utilized as described in the Materials and Methods. The HO-1 mRNA expression was increased ~23-fold at 4 h (data not shown) and ~30-fold at 8 h following glycerol injection in HO-1$^{+/+}$ kidneys (Figure 5a). In contrast, hHO-1 BAC kidneys revealed ~5- and ~14-fold increase in HO-1 mRNA expression at 4 h (data not shown) and 8 h, respectively, after glycerol administration (Figure 5b). HO-1 protein and HO enzyme activity showed higher basal levels in the hHO-1 BAC kidneys compared with the HO-1$^{+/+}$ mice, and this increase was even higher following glycerol-induced rhabdomyolysis at 16 h (Figure 5c and d). Survival rate and serum creatinine level of each group of mice were monitored to determine the protective effects of the human *HO-1* gene in hHO-1 BAC mice after glycerol-induced rhabdomyolysis. All HO-1$^{-/-}$ mice died within 4 days after glycerol injection with markedly increased serum creatinine. In all, 90% of HO-1$^{+/+}$ mice and 100% of hHO-1 BAC mice survived for 10 days after injection without significant changes in serum creatinine levels, suggesting that the human *HO-1* gene and product in hHO-1 BAC mice remains functional (Figure 5e and f).

To further examine the response of HO-1$^{+/+}$ and hHO-1 BAC transgenic mice in a model of non-heme-mediated renal injury, we tested the effects of cisplatin nephrotoxicity in

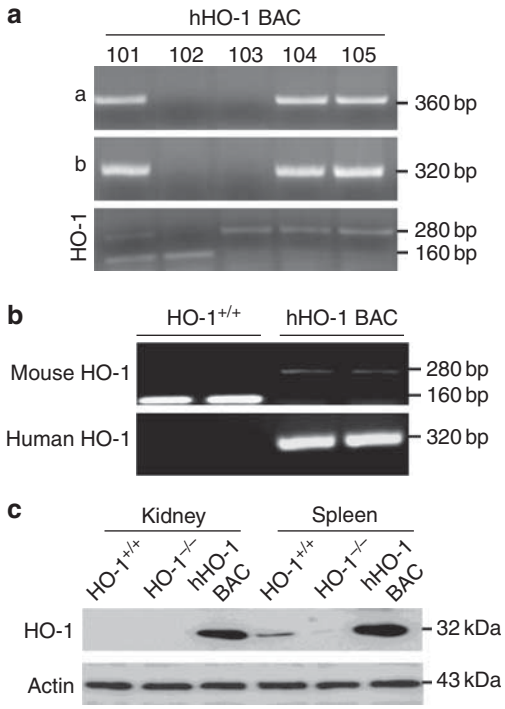

Figure 3 | Generation and characterization of 'humanized' heme oxygenase-1 bacterial artificial chromosome (hHO-1 BAC) mice. (**a**) Five transgenic mice were obtained from a pair of HO-1$^{+/-}$ BAC-positive mice. Primers for HO-1 BAC (a and b, see Table 1 and Figure 1a) were used to screen whether they were positive for HO-1 BAC. Mice were also genotyped using a combination of primers for the detection of mouse *HO-1* gene (lower 160-bp band) and/or neomycin cassette (upper 280-bp band) inserted in order to generate HO-1$^{-/-}$ mice (Table 1). (**b**) Genomic DNA was used to evaluate the presence of mouse and human HO-1. Whereas the genotyping of HO-1$^{+/+}$ mice reveals a single band at 160 bp for mouse HO-1, the absence of mouse HO-1 in hHO-1 BAC mice gives a single band at 280 bp, denoting the presence of the neomycin cassette derived from the HO-1$^{-/-}$ mice. A heterozygote would reveal two bands at 160 and 280 bp. The presence of human HO-1 in hHO-1 BAC mice is confirmed by using a human-specific primer that yields a 320-bp band. (**c**) Microsomal fractions of kidney and spleen from HO-1$^{+/+}$, HO-1$^{-/-}$, and hHO-1 BAC mice were isolated and analyzed by immunoblot for HO-1 expression. The blot was stripped and reprobed with anti-actin antibody for a loading control.

these mice. We have previously reported that HO-1 is induced in this model and is a protective response.[12] As expected, HO-1 mRNA and protein and enzyme activity were increased in HO-1$^{+/+}$ mice after cisplatin administration (Supplementary Figure S2A, C and D online). hHO-1 BAC mice displayed significant increases in HO-1 mRNA (~3.5-fold at 6 h; Supplementary Figure S2B online), HO-1 protein (~2.2-fold at 12 h; Supplementary Figure S2C online), and HO enzyme activity (~2.2-fold at 24 h; Supplementary Figure S2E online) compared with basal levels. These data demonstrate that even though basal levels of HO-1 are elevated in the hHO-1 BAC mice, HO-1 is significantly inducible in another disease setting (for example, cisplatin nephrotoxicity), consistent with the rhabdomyolysis model. In addition, renal function measured by serum creatinine was markedly preserved in the hHO-1 BAC mice compared with HO-1$^{+/+}$ mice following cisplatin administration (Supplementary Figure S2F online).

Molecular mechanisms of the human HO-1 gene transcription *in vivo*

We have previously shown the importance of USF1/2 and Sp1 in regulating hemin-mediated HO-1 expression in renal epithelial cells *in vitro*.[33,35,36] To examine the *in vivo* relevance of the *in vitro* findings, we performed chromatin immunoprecipitation (ChIP) assay to determine the association of the indicated transcription factors with regulatory regions in the *HO-1* gene in kidneys of the hHO-1 BAC transgenic mice subjected to rhabdomyolysis (Figure 6). Upon induction of HO-1, JunB, Sp1, USF1, and USF2 were associated with the −4.5 kb promoter region that contains the DNase I hypersensitive site (HS), HS-2.[35] However, JunD did not show any association to the promoter region (Figure 6a). For the 220-bp intronic enhancer region, maximal binding was observed with Sp1, to a lesser extent with JunB, USF1, and USF2, and no binding with JunD (Figure 6b). The +2.2 kb region of the human *HO-1* gene was used as a negative control and none of the tested transcription factors were associated with this region (Figure 6c).

CCCTC-binding factor (CTCF) is a multifunctional transcription factor that is a master controller of several genes by regulating activation, repression, insulation, and silencing.[39–44] Interestingly, one of the major mechanisms of CTCF-mediated transcriptional regulation is the formation of chromatin looping.[41,45] We tested if CTCF was bound to various regulatory regions in the kidneys of hHO-1 BAC mice following rhabdomyolysis. ChIP assay showed that CTCF associates with the proximal E-box, −4.5 kb promoter, and 220 bp intronic enhancer but not the +2.2 kb region upon induction of the human *HO-1* gene *in vivo* (Figure 6d).

In vivo chromatin looping occurs in hHO-1 BAC mice for induction of human *HO-1* gene transcription

Chromatin looping was studied in hHO-1 BAC mice using the chromosome conformation capture (3C) assay upon induction of HO-1 transcription after glycerol-induced rhabdomyolysis. Mice were injected with 50% glycerol or saline (negative control) and kidneys were removed after 3 h for the 3C assay. *Bgl*II restriction enzyme was used to determine the interaction of fragments containing the 220-bp enhancer and the −4.5 kb promoter as described in the map in Figure 6e. As shown in Figure 6f, a 7.5-fold increase of crosslinking efficiency was detected between the enhancer containing fragment with the −4.5 kb region after induction of rhabdomyolysis compared with saline-injected mice. These results demonstrate the pivotal role of USF1, CTCF, and Sp1 in regulating *HO-1* gene expression *in vivo* via chromatin looping.

USF1/2, Sp1, and CTCF regulate chromatin loop formation

Overexpression of USF1 and/or USF2 as well as Sp1 induced endogenous HO-1 protein and mRNA *in vitro*. In addition,

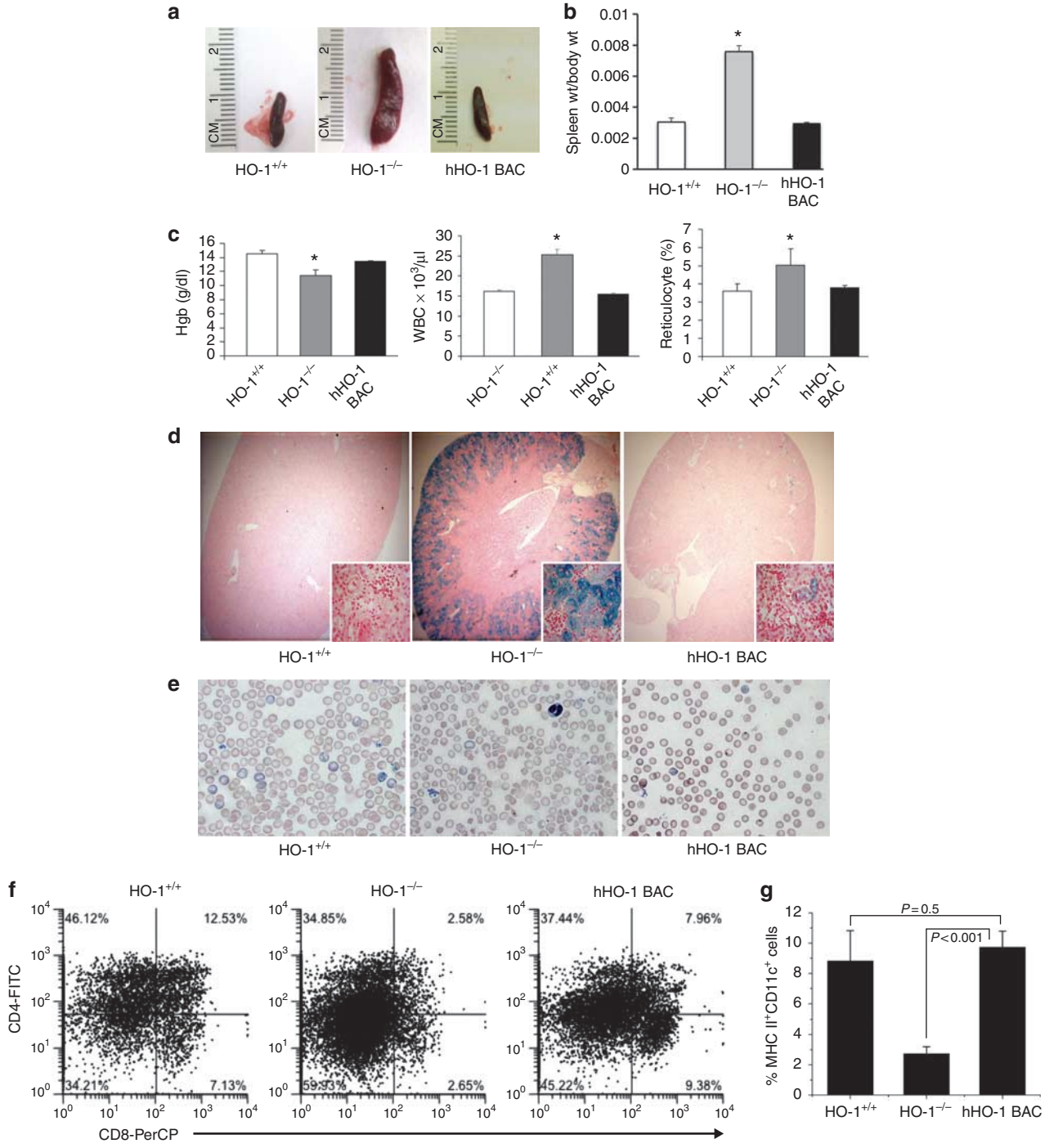

Figure 4 | Human heme oxygenase-1 (HO-1) in hHO-1 bacterial artificial chromosome (BAC) transgenic mice rescues the pathological phenotype of HO-1$^{-/-}$ mice. Spleens from 25- to 35-week-old HO-1$^{+/+}$ ($n=8$), HO-1$^{-/-}$ ($n=7$), and hHO-1 BAC ($n=7$) transgenic mice were collected and their (**a**) lengths and (**b**) weights (wt) were compared. Weights of spleen were normalized to body weight of each animal, and average normalized values were plotted for each group (mean ± s.e.m.). *$P<0.05$ vs. HO-1$^{+/+}$ and hHO-1 BAC mice. (**c**) Whole blood from 30- to 40-week-old HO-1$^{+/+}$, HO-1$^{-/-}$, and hHO-1 BAC mice were collected and hemoglobin (Hgb), leukocyte (white blood cell (WBC)), and reticulocyte counts were measured ($n=4$–5 per group). *$P<0.05$ vs. HO-1$^{+/+}$ and hHO-1 BAC mice. (**d**) Kidneys from 25- to 35-week-old HO-1$^{+/+}$, HO-1$^{-/-}$, and hHO-1 BAC mice were collected and Prussian blue staining was performed to detect tissue iron in paraffin-embedded sections. (**e**) Peripheral blood smears were prepared from HO-1$^{+/+}$, HO-1$^{-/-}$, and hHO-1 BAC mice and stained using Wright-Giemsa staining to determine red blood cell (RBC) morphology. (**f**, **g**) Subsets of splenic dendritic cells (DCs) from HO-1$^{+/+}$, HO-1$^{-/-}$, and hHO-1 BAC transgenic mice were compared as described in the Materials and Methods. CD8 and CD4 expression is shown on CD11c and major histocompatibility complex class II (MHC II)-gated cells from each group of mice (**f**). Numbers within graph quadrants depict the percentage of CD11c$^+$MHC II$^+$-positive cells. The histogram shown depicts the average from three animals in the percentage of CD8$^+$ DCs among the population of CD11c$^+$MHC II$^+$ DCs.

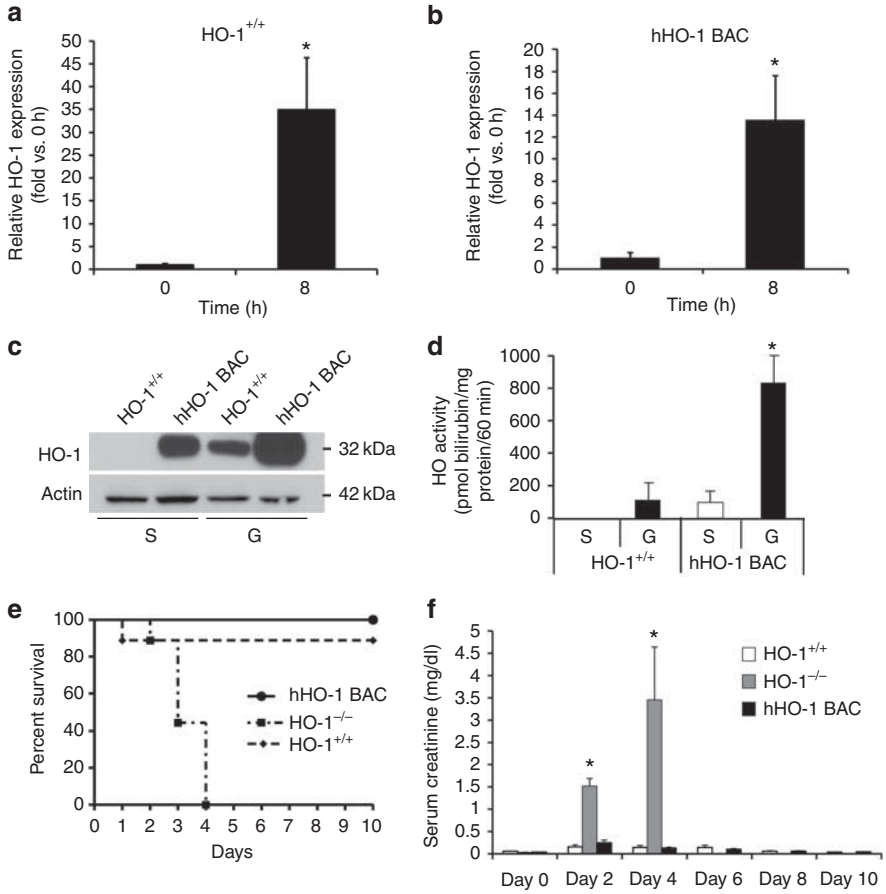

Figure 5 | Heme oxygenase-1 (HO-1) expression is induced at higher levels after rhabdomyolysis in humanized HO-1 bacterial artificial chromosome (hHO-1 BAC) mice. Rhabdomyolysis was induced by injecting 50% glycerol (7.5 ml/kg body weight) in HO-1$^{+/+}$ and hHO-1 BAC mice (**a** and **b**, respectively; $n = 9$ per group). Kidneys from HO-1$^{+/+}$ and hHO-1 BAC mice were collected and total RNA was isolated. At 8 h after glycerol administration, HO-1 was induced ~30-fold in (**a**) HO-1$^{+/+}$ kidneys, whereas the (**b**) hHO-1 BAC kidneys revealed ~14-fold HO-1 induction. *$P < 0.01$. (**c**) Microsomal fractions from kidneys of HO-1$^{+/+}$ and hHO-1 BAC mice after injection of saline (S) as a control and 50% glycerol (G) for 16 h were analyzed for HO-1 protein expression using western analysis. Note that normalization of the band intensity to corresponding actin levels shows no significant difference between glycerol-treated HO-1$^{+/+}$ and hHO-1 BAC saline-treated mice. (**d**) Kidneys of HO-1$^{+/+}$ and hHO-1 BAC mice after injection of saline (S) and glycerol (G) were collected and HO enzyme activity was measured at 16 h after glycerol administration as described in the Materials and Methods ($n = 3$ per group). *$P < 0.05$ vs. HO-1$^{+/+}$. (**e**) Survival rate was monitored after induction of rhabdomyolysis in HO-1$^{+/+}$, HO-1$^{-/-}$, and hHO-1 BAC mice ($n = 10$ per group). Experiments were ceased 10 days after injection. (**f**) Serum creatinine was measured in HO-1$^{+/+}$, HO-1$^{-/-}$, and hHO-1 BAC mice after indicated days after induction of rhabdomyolysis.

hemin induction of HO-1 resulted in increased endogenous Sp1 expression, but the levels of USF-1 and USF-2 were unchanged. ChIP assays showed that USF1 associated with the −4.5 kb HS-2, proximal E-box, and 220-bp intronic enhancer regions upon induction of HO-1 by hemin (Supplementary Figure S3 online). 3C assay demonstrated that USF1 overexpression facilitated chromatin loop formation between the −4.5 kb promoter region (HS-2) and the 220-bp intronic enhancer (Supplementary Figure S4A online). Similarly, the proximal E-box interacted with the −4.5 kb promoter via chromatin looping (Supplementary Figure S4B online). Further confirmation of chromatin loop formation was achieved using the ChIP-loop assay.[46–48] Cells were treated with 5 μmol/l hemin for 3 h to induce HO-1 transcription and ChIP-loop assay was performed using the *Bgl*II restriction enzyme along with anti-Sp1 and anti-USF-1 antibodies to precipitate crosslinked DNA–protein complex. We demonstrate that for the interaction between the −4.5 kb promoter (HS-2) and the 220-bp intronic enhancer, Sp1 and USF-1 are involved in the process of chromatin looping and subsequent HO-1 transcription (Supplementary Figure S4C online).

In order to determine if CTCF is involved in HO-1 transcription and related with other transcription factors, we performed ChIP assay using anti-CTCF antibody for the proximal E-box, −4.5 kb promoter, and 220-bp intronic enhancer regions. CTCF bound to all three regions tested upon induction of HO-1 by hemin treatment (Supplementary Figure S5A online). Hemin-mediated HO-1 induction caused the binding of RNA *Pol*II to proximal E-box, −4.5 kb promoter, and 220-bp intronic enhancer regions, but no association was detectable with the +2.2 kb region that also

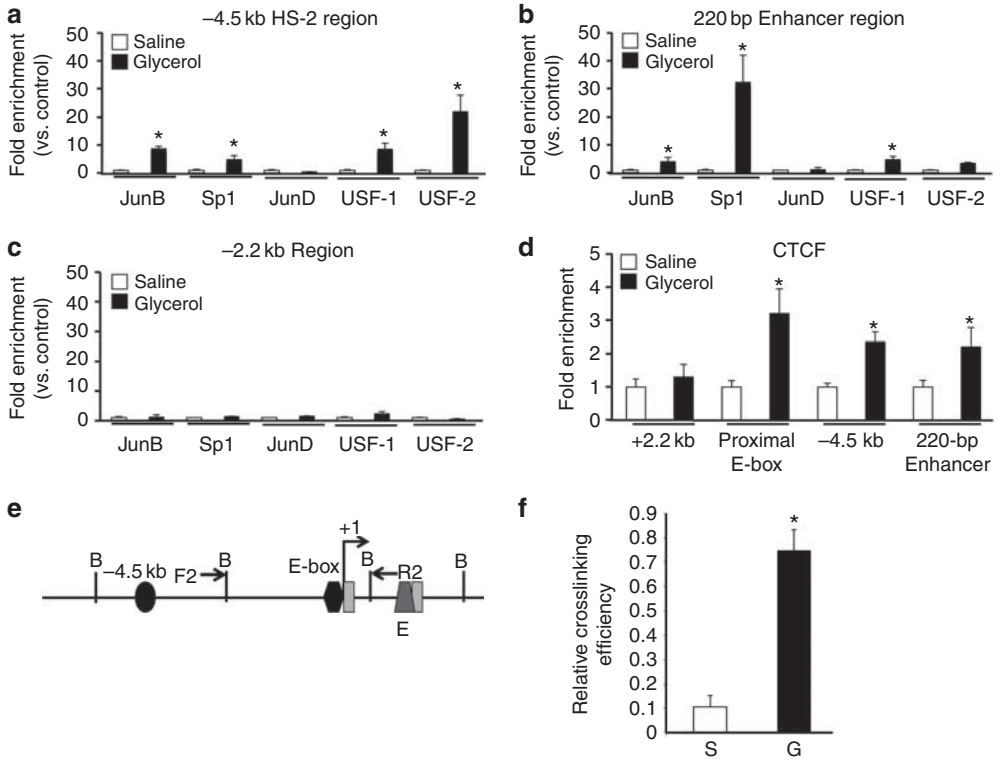

Figure 6 | Glycerol-induced rhabdomyolysis induces chromatin-looping-mediated promoter-enhancer interaction and increases binding of JunB, Sp1, USF1/2, and CTCF to regulatory regions of the human *heme oxygenase-1* (*HO-1*) gene *in vivo*. (**a**–**c**) hHO-1 BAC transgenic mice were injected with 7.5 ml/kg body wt 50% glycerol (G) or saline (S) and kidneys were harvested after 3 h. An *in vivo* ChIP assay was performed to determine changes in association of indicated transcription factors within the (**a**) −4.5 kb human HO-1 promoter region , (**b**) 220-bp intronic enhancer region, and (**c**) the + 2.2 kb internal E-box region as a negative control as described in the Materials and Methods. Results represent three independent experiments and fold enrichment vs. saline-injected mice are shown (mean ± s.e.m.). (**d**) Kidneys from hHO-1 BAC transgenic mice injected with 50% glycerol or saline were harvested and *in vivo* ChIP was performed to determine the association of CTCF with −4.5 kb promoter, 220-bp enhancer, and proximal E-box regions. The + 2.2 kb E-box region was used as negative control. Results represent two independent experiments and relative fold enrichments vs. saline-injected mice are shown (mean ± s.e.m.). *$P < 0.05$ vs. saline-treated hHO-1 BAC mice. (**e**) Map of the human HO-1 promoter, where B denotes *Bgl*II restriction sites flanking the −4.5 kb promoter regions, proximal E-box elements, and 220-bp enhancer (E). Arrows denote primers used for 3C assay. Gray rectangles indicate exons in the human *HO-1* gene. (**f**) hHO-1 BAC mice were injected with glycerol (G) and saline (S) for 3 h and kidneys were harvested. 3C assay was performed to determine the interaction between −4.5 kb promoter and 220-bp enhancer (F2/R2) using *Bgl*II restriction enzyme. Interactions between promoter and enhancer regions were determined and quantified as relative crosslinking efficiency. Results shown are from three independent experiments (mean ± s.e.m.). *$P < 0.05$ vs. saline-injected hHO-1 BAC mice. 3C, chromosome conformation capture; BAC, bacterial artificial chromosome; ChIP, chromatin immunoprecipitation; CTCF, CCCTC-binding factor; hHO-1 BAC, humanized HO-1 BAC; HS-2, hypersensitive site 2; Sp1, specificity protein 1; USF1 and 2, upstream stimulatory factors 1 and 2.

contains an E-box sequence (Supplementary Figure S5A and 5B online).

DISCUSSION

In this study, we report a novel *in vivo* model for studying the functional and regulatory mechanisms of the human *HO-1* gene via the generation of hHO-1 BAC transgenic mice. The integration of human HO-1 successfully rescued the phenotype of the HO-1$^{-/-}$ mice, demonstrating the integrity and functional role of the human HO-1 transgene and its gene product. Furthermore, the results of the current studies using rhabdomyolysis-induced kidney injury in hHO-1 BAC mice demonstrate the complex changes in chromatin conformation and loop formation *in vivo*, providing important insights to the molecular regulation of human *HO-1* gene expression. The studies have also identified for the first time, the involvement of CTCF, a master regulator in *HO-1* gene expression *in vitro* and *in vivo*.

HO-1 mitigates cellular injury by exerting anti-oxidant, anti-apoptotic, and anti-inflammatory effects.[31,49–51] Because of the beneficial and protective effects of HO-1 in several pathological states, developing an appropriate *in vivo* model for the study of the molecular mechanism of HO-1 expression is imperative. Unlike other currently available *in vivo* models to study the biological aspects of human HO-1, HO-1 BAC transgenic mice can be used to study the intricate molecular mechanisms that control human *HO-1* gene transcription. HO-1 BAC mice showed global HO-1 mRNA and protein overexpression in multiple tissues. Interestingly, the pattern of expression closely mimicked the sites where

HO-1 would otherwise be inducible following tissue injury. In the kidney, HO-1 expression was seen in the proximal tubules, a site where HO-1 is induced in models of acute kidney injury.[52] In the liver, HO-1 expression was detected in Kupffer cells. Consistent with this observation is the finding that Kupffer cell–depleted mice fail to show resection-induced increase of HO-1, suggesting that the major hepatic cell type that accounts for HO-1 expression in liver is the Kupffer cell.[53,54] In the brain, astrocytes were the predominant cell type with increased HO-1 expression in the HO-1 BAC mice. Hypoxia-induced HO-1 expression in the brain results in increased HO-1 levels in astrocytes, but not in the microglia.[55] Our results also demonstrate that increases in HO enzyme activity confirm the global overexpression and active nature of the inserted *HO-1* gene in the BAC mice. In addition, the body weight and lifespan of HO-1 BAC mice and HO-1$^{+/+}$ did not show any major differences, indicating that the integrated human *HO-1* gene did not cause any significant physiological derangements in the transgenic mice.

More importantly, we demonstrate that the inserted human *HO-1* gene is functional and rescues the pathological phenotype of the HO-1$^{-/-}$ mice. HO-1$^{-/-}$ mice have reduced live births and partial embryonic lethality, which were reversed in the hHO-1 BAC mice. Splenomegaly, anemia, DC abnormalities, and tissue iron deposition seen in HO-1$^{-/-}$ mice were normalized in the hHO-1 BAC mice. HO-1$^{-/-}$ mice are highly sensitive to rhabdomyolysis-induced acute kidney injury,[17] and hHO-1 BAC mice showed markedly improved survival and preserved renal function. hHO-1 BAC mice were also protected in a model of cisplatin-induced nephrotoxicity. Interestingly, RBCs of the HO-1 BAC and the hHO-1 BAC mice contained increased number of inclusions that appeared similar to Howell–Jolly bodies. Despite the fact that Howell–Jolly bodies are generally considered a hallmark of asplenia, the physical appearance of the spleens of hHO-1 BAC mice as well as their weights were not significantly different from the HO-1$^{+/+}$ spleens. This observation is intriguing and deserves further investigation.

Our studies using hHO-1 BAC mice support previous *in vitro* evidence for chromatin looping as a mechanism for regulation of the human *HO-1* gene. Transcription factors, Sp1, USF1/2, and JunB, were identified as positive regulators for human HO-1 expression and our results indicate that they are associated with the same regulatory regions and involved in chromatin looping. These studies have also identified a pivotal role for the transcription factor, CTCF, in the regulation of human *HO-1* gene expression. Sp1 is a transcription factor that plays an important role in the regulation of a number of genes. It has a zinc-finger protein motif by which it may bind to DNA, enhancing the transcription of the specific gene. In contrast, CTCF belongs to a family of proteins known as chromatin insulators. These proteins are suggested to form domains within which specific enhancer-gene interactions may occur. Mounting evidence suggests that CTCF may bind to distant sites or even different chromosomes, thereby allowing chromatin looping and transcriptional regulation.

The hHO-1 BAC transgenic mice are invaluable *in vivo* models for studying not only the function but also the regulation of the human *HO-1* gene. hHO-1 BAC mice can be used to better understand how the human *HO-1* gene is induced and protects against various disease states such as acute kidney injury, atherosclerosis, sepsis, vascular restenosis, organ transplantation, as well as others. Moreover, for the study of transcriptional regulation of human *HO-1* gene, the hHO-1 BAC mouse containing the complete human *HO-1* gene with all its regulatory elements would be a prerequisite for better elucidation of the mechanisms underlying *HO-1* gene expression. Additionally, the absence of the mouse *HO-1* gene in hHO-1 BAC mice removes any confounding effects from endogenous HO-1, allowing all outcomes to be attributed to the human *HO-1* gene. It is important to note that the humanized HO-1 mouse described herein depends on transcription factors that are of murine origin. However, significant ($>90\%$) homology exists between the transcription factors of the two species and obviates this limitation. Another advantage of the humanized transgenic mouse model is the potential for testing of novel small molecular agents that could be evaluated in future therapeutic applications.

On the other hand, we acknowledge that there are certain limitations of this mouse model. Most importantly, the basal levels of HO-1 are significantly higher in hBAC mice compared with HO-1$^{+/+}$ mice. This may be because of the insertion of the BAC DNA into the euchromatin region. Another possible explanation is the absence of human-specific inhibitory regulators (for example, microRNAs) in the mouse environment. These are currently being investigated in our laboratory. However, our results show that HO-1 mRNA is significantly induced ($\sim$5-fold and 14-fold at 4 and 8 h, respectively) in hBAC mice in the rhabdomyolysis model. Moreover, HO-1 protein levels and HO enzyme activity are significantly higher ($\sim$3.5-fold and $\sim$8-fold, respectively) than control levels in the glycerol model (Figure 5d). Inducibility of HO-1 mRNA and protein and enzyme activity was also confirmed in cisplatin-induced nephrotoxicity, a non-heme-dependent model of acute kidney injury (Supplementary Figure S2 online). These results indicate that although in the basal state hBAC mice express a higher level of HO-1, there is still capacity for significant inducibility and thereby allowing for investigation of the human *HO-1* gene in pathological conditions.

In summary, humanized HO-1 BAC transgenic mice are able to rescue the phenotype of HO-1$^{-/-}$ mice, and transcription factors including JunB, Sp1, USF1/2, and CTCF regulate transcription of the human *HO-1* gene via chromatin looping *in vivo*. The hHO-1 BAC transgenic mice can be utilized as an *in vivo* model to better elucidate the functional significance and molecular regulation of the human *HO-1* gene.

MATERIALS AND METHODS

Reagents

Tissue culture media and supplements were obtained from Mediatech (Manassas, VA). Rabbit or mouse polyclonal antibodies against USF1 (SC-229), USF2 (SC-862), Sp1 (SC-14027), JunB (SC-8051), and JunD (SC-74) were from Santa Cruz Biotechnology (Santa Cruz, CA). Anti HO-1 (SPA-895) and HO-2 (SPA-897) antibody was from Stressgen (Plymouth Meeting, PA). Restriction endonucleases for chromosome conformation capture were obtained from New England Biolabs (Beverly, MA). Lipofectamine for transient transfection was purchased from Invitrogen (Carlsbad, CA).

Cell culture, plasmids, and transfection

Human embryonic kidney 293 (HEK293) cells (ATCC, Manassas, VA) were grown in Dulbecco's modified Eagle's medium/F12 medium (Mediatech) supplemented with 10% fetal bovine serum, 0.1 mmol/l nonessential amino acids, 1 mmol/l sodium pyruvate, and 1.5 mg/ml sodium bicarbonate. Cells were grown at 37 °C in 95% air and 5% CO_2.

The plasmid constructs for USF1 (psvUSF1), USF2 (psvUSF2), and pRc/CMV566 were gifts from Dr M Sawadogo (University of Texas at Houston, Houston, TX). The dominant-negative expression vector for USF, hemagglutinin-tagged A-USF, was kindly provided by Dr C Vinson (National Cancer Institute, National Institutes of Health, Bethesda, MD). The Sp1 expression vector was kindly provided by Kun-Sang Chang (University of Texas MD Anderson Cancer Center, Houston, TX) and has been described elsewhere.[56]

HEK293 cells at a confluence of 60–70% were grown in 10 cm tissue culture dishes and were transiently transfected with equimolar amounts of plasmids using Lipofectamine 2000 (Invitrogen) according to the manufacturer's instructions. Transfected cells were allowed to recuperate for indicated time periods before harvesting.

Generation of HO-1 BAC transgenic mice

The HO-1 BAC clone (GenBank accession number: Z82244; 87,869 bp) containing the human *HO-1* gene along with the 3′ end of the *TOM1* gene and the *MCM5* gene was obtained from Sanger Institute (Cambridge, UK). The HO-1 BAC was purified for injection using the QIAGEN Large-construct kit (QIAGEN, Valencia, CA). The BAC was quantified using agarose gel electrophoresis, and sets of 200 C57BL6/J oocytes were microinjected with 30 ng of the purified BAC DNA at the UAB Transgenic Mouse Core facility. Fertilized ova were subsequently implanted into pseudopregnant females and offspring were analyzed for the insertion of the HO-1 BAC. Two independent founder lines were produced that transmitted the transgene and genotyped with DNA extracted from tails, followed by subsequent PCR amplification of four different regions within the HO-1 BAC (Figure 1a) using primers shown in Table 1. Integration of HO-1 BAC was demonstrated by Southern blot analysis after digestion of tail DNA with *Eco*RI and hybridization with the probe generated from PCR amplicon (primer pair b), which resulted in a single band at 8 kb (Figure 1c). The inserted BAC DNA contains the entire human *HO-1* gene along with all of its regulatory regions. Hence, all experiments that involved hHO-1 BAC mice examine the full-length human *HO-1* gene. All animal studies were approved by our institutional animal care and use committee.

Copy number estimation of transgenic mice

Copy number estimates were derived from ΔCt values for standard curve samples that mimic the genetic integration of the transgene. Serially diluted purified HO-1 BAC DNA were mixed with 200 ng of mouse genomic DNA and used as standards. In order to calculate ΔCt values, the average of duplicate Ct values generated with the HO-1 BAC probe (Table 1) was subtracted from the average Ct value of mouse *prolactin* (*Prl*) gene, which represents two copies. Then, ΔCt values from genomic DNA of transgenic mice were calculated using BAC and *Prl* probes as in standard samples. ΔΔCt values were calculated by comparing two ΔCt values and copy number was calculated.

Conventional cytogenetic and FISH analyses

The HO-1 BAC was labeled in SpectrumOrange using the Abbott nick translation kit (Abbott Molecular, Des Plaines, IL) and used as a FISH probe. The probe was validated by metaphase FISH analysis on 20 human metaphase peripheral blood cells to confirm that it hybridizes to chromosome 22 band q12.3 (*HMOX1* gene) with no cross-hybridization elsewhere in the human genome (Figure 1d, left panel). Interphase FISH analyses were then performed on peripheral blood cells from both the wild type (non-transgenic; Figure 1d, middle panel) and transgenic mice using the HO-1 probe (Figure 1d, right panel). Slide hybridization and washes were performed using standard FISH protocols. The slides were then counterstained with 4,6-diamidino-2-phenylindole and analyzed with an Olympus BX61 microscope (Olympus America, Melville, NY) equipped with the appropriate filter combination and a CCD camera, and coupled to the CytoVision image analysis system (Applied Imaging, Santa Clara, CA). A total of 100 interphase cells were analyzed from each mouse. G-banded chromosome analysis was performed on metaphase spreads prepared from unstimulated bone marrow cell cultures from the transgenic mice using standard techniques. The chromosomes were analyzed and karyotyped using the CytoVision image analysis system (Applied Imaging).

Real-time PCR

Total RNA was isolated from cells or tissues by TRIzol (Invitrogen), and SYBR Green-based real-time PCR was performed on cDNA first-strand synthesis products generated from total RNA (Invitrogen). The reactions were performed in triplicate. Relative mRNA expression was quantified using the ΔΔCt method and GAPDH (glyceraldehyde 3-phosphate dehydrogenase) was used as an internal control. Real-time primers are described in Table 1. For copy number estimation of transgenic mice, custom TaqMan probe for BAC and *Prl* gene (control) were used. The primers for BAC were same as the primers used for genotyping of transgenic mice (BAC b, c, and d; Table 1) and sequences of *Prl* primers and probes are listed in Table 1.

Western blot analysis

Harvested cells or collected tissues were lysed in RIPA buffer (50 mmol/l Tris/HCl, 1% NP-40, 0.25%. deoxycholic acid, 150 mmol/l NaCl, 1 mmol/l EGTA, 1 mmol/l sodium orthovanadate, and 1 mmol/l sodium fluoride) with protease inhibitor (Roche Applied Science, Indianapolis, IN) and quantified using BCA protein assay (Thermo Scientific, Rockford, IL). Total protein (10–15 μg) was resolved on a 12% Tris-glycine sodium dodecyl sulfate polyacrylamide gel electrophoresis. After transfer to a polyvinylidene fluoride membrane (Millipore, Billerica, MA), HO-1, HO-2, and actin were detected using 1:5000 dilutions of primary rabbit polyclonal antibodies, followed by a horseradish peroxidase–conjugated anti-rabbit IgG. The antibody used to detect HO-1 is a polyclonal antibody that recognizes HO-1 of both species with the

same intensity. Protein was visualized using the enhanced chemiluminescence detection system (GE Healthcare, Piscatway, NJ).

Measurement of HO enzyme activity

Tissue was homogenized in 3 ml of buffer (200 mmol/l KH_2PO_4, 135 mmol/l KCl, 0.1 mmol/l. EDTA, pH 7.4), and then sonicated three times for 5 s at 4 °C. The samples were centrifuged (10,000 × *g*, 4 °C, 20 min). The supernatant was transferred to ultracentrifuge tubes, followed by an ultracentrifugation (100,000 × *g*, 4 °C, 60 min; Beckman L7–35 Ultracentrifuge, 70 Ti rotor, Indianapolis, IN). The microsomal pellet was resuspended in 320 µl of HO enzyme activity buffer (100 mmol/l KH_2PO_4, 2 mmol/l $MgCl_2$, pH 7.4). After sonication (three times for 5 s each at 4 °C), the supernatant was used to determine HO enzyme activity in a reaction mixture containing rat liver cytosol (as a source of biliverdin reductase, 2 mg/assay), hemin (20 µmol/l), glucose-6-phosphate (2 mmol/l), glucose-6-phosphate dehydrogenase (0.2 U), and nicotinamide adenine dinucleotide phosphate (0.8 mmol/l) in a total volume of 400 µl. After the reaction was incubated at 37 °C for 60 min in the dark, the formed bilirubin was extracted with 1 ml of chloroform by vigorous vortexing three times for 10 s. After centrifugation (1000 × *g*, 5 min, room temperature), optical density at 464 and 530 nm of the organic phase was determined and HO enzyme activity was calculated and expressed as fold increase versus controls.

Immunohistochemistry

Tissues were removed and fixed in 10% formalin for 24 h and dehydrated in 70% ethanol before embedding in paraffin. Paraffin-embedded tissues were cut into 4 µm sections, and then deparaffinized and rehydrated using Citrisolv (d-limonene-based solvent) and isopropanol, respectively. Retrieval of antigen for anti-HO-1 was performed by steaming in Trilogy solution. Sections were blocked with 5% normal goat serum for 20 min, and then incubated for 16 h at 4 °C with polyclonal rabbit anti-HO-1 antibody (SPA-896, Stressgen) diluted 1:1000 in phosphate-buffered saline (PBS) with 0.1% Tween-20. Peroxidase-conjugated goat anti-rabbit antibody was applied for 1 h at room temperature, followed by PBS washes. VIP substrate kit (Vector Laboratories, Burlingame, CA) was prepared following the manufacturer's protocol and applied for 3 min. Tissues were dehydrated using ethanol and xylene and mounted. For the study of HO-1 expression pattern in kidney, serial paraffin-embedded tissue sections were incubated with biotinylated lotus lectin (Vector Laboratories) or anti-HO-1 as described earlier.[57] Images were captured using a Leica DM IRB microscope (Leica Microsystems, Bannockburn, IL) and Image-Pro Plus software (Media Cybernetics, Bethesda, MD).

Splenic DC preparation

Spleens from HO-1$^{+/+}$, HO-1$^{-/-}$, and hHO-1 BAC mice were harvested, cut into small fragments, minced, and digested with 100 U/ml collagenase D (Roche Diagnostics, Indianapolis, IN) containing Dulbecco's PBS (Invitrogen, Grand Island, NY) solution and incubated for 20 min at room temperature. EDTA was added (final concentration, 0.1 mol/l) to disrupt DC/T cell complexes and incubated for 5 min. Cells were filtered through a 70-µm stainless still sieve (BD Falcon; BD Biosciences, Bedford, MA) for removing undigested fibrogenous materials and centrifuged at 300 × *g* for 10 min. Supernatants were removed, and RBCs were lysed using buffered ammonium chloride lysis solution. After cells were washed in PBS, they were used for experiments.

Flow cytometry

Cells were washed once with cold PBS and were incubated for 10 min at room temperature with anti-mouse CD16/32 (eBioscience, San Diego, CA) to block nonspecific binding to FCγ3 receptors. Cells were initially stained with fluorescein isothicyanate–conjugated anti-mouse CD86 (clone GL-1), phycoerythrin-conjugated anti-mouse CD19 (clone 1D3), anti-mouse CD11c biotin (clone HL3), and allophycocyanin-conjugated anti-mouse major histocompatibility complex class II (MHC II) (clone M5/114.15.2) for 30 min on ice. Cells were washed and stained with peridinin chlorophyll protein complex−conjugated anti-mouse streptavidin for additional 30 min on ice. Phycoerythrin-conjugated, fluorescein isothicyanate–conjugated, and allophycocyanin-conjugated isotype-matched antobodies of irrelevant specificity were used as controls. DC subsets were identified by incubation with fluorescein isothicyanate–conjugated, phycoerythrin-conjugated, peridinin chlorophyll protein complex-conjugated, and allophycocyanin-conjugated monoclonal antibody specific for CD11c, CD4, CD8, and MHC II, respectively. Data acquisition was performed on a FACSCalibur flow cytometer (BD Biosciences), and results were analyzed using Winlist Software (Verity Software House, Topsham, MA).

Hematological assays

Peripheral blood smears were prepared using a drop of blood from the mouse tail. Slides were submerged in methanol for 1 min followed by Wright-Giemsa Fuccillo stain (Harleco, Lawrence, KA) for 5 min as described.[58] Slides were then transferred into 300 ml of the Giemsa solution containing 80 ml Wright-Giemsa stain, 50 ml phosphate buffer, pH 6.8, and 170 ml distilled water for 10 min. Slides were washed in phosphate buffer (pH 6.8) for 3 min followed by deionized water for 3 min. Slides were then dried at room temperature and covered with cover slips using mounting medium xylene (Fisher Scientific, Pittsburgh, PA).

For other hematologic indices, peripheral blood was collected from anesthetized mice into Microtainer EDTA collection tubes (BD Biosciences, Franklin Lakes, NJ). Hemoglobin concentrations were determined after conversion to cyanmethemoglobin by lysing RBCs in Drabkin reagent (Sigma-Aldrich, St Louis, MO), removing insoluble RBC membranes by centrifugation, measuring the absorbance at 540 nm on a spectrophotometer, and comparing with hemoglobin standards. Reticulocyte counts were determined by flow cytometry after staining with thiazole orange as described elsewhere.[59]

Chromosome conformation capture

3C assay was performed according to the method described earlier.[60,61] Briefly, transiently transfected HEK293 cells were recovered for 24 h. Cells were washed with PBS twice and 2% formaldehyde was added to the cells for 10 min at room temperature for crosslinking. For *in vivo* 3C assay, kidneys from hHO-1 BAC transgenic mice injected with saline (control) or 50% glycerol to induce rhabdomyolysis at 3 h after injection were collected and diced into small pieces (between 1 and 3 mm^3). Then, 1% formaldehyde was added to the tissue for 20 min at room temperature for crosslinking. The crosslinking was terminated by adding 2.5 mol/l glycine to a final concentration of 0.125 mol/l for 10 min at 4 °C and then samples were centrifuged at 100 × *g* for 2 min. After washing, cells or tissues were disaggregated by using Dounce homogenizer. Crosslinked cells were washed with cold PBS and lysed for 1 h with ice-cold lysis buffer containing 10 mmol/l Tris (pH 8.0), 10 mmol/l

NaCl, 0.2% NP-40, and 1 mmol/l dithiothreitol. The nuclei of the cells were then harvested and suspended in the appropriate restriction enzyme buffer containing 0.3% SDS and incubated at 37 °C for 1 h with gentle shaking. SDS was then sequestered from the samples by the addition of 1.8% Triton X-100 (Fisher Scientific) and the samples were incubated at 37 °C for 1 h. The samples were digested with either *Bgl*II or *Sph*I restriction enzyme (New England Biolabs) at 37 °C for 16 h. Restriction enzymes were inactivated by the addition of 1.6% SDS and further incubation at 65 °C for 20 min. Samples were diluted with T4 DNA ligase buffer (New England Biolabs) to achieve ~3 ng of DNA/μl, then 200 U T4 DNA ligase (New England Biolabs) was added and incubated for 4 h at 16 °C. Samples were then incubated with Triton X-100 followed by incubation with Proteinase K (200 μg/ml) at 65 °C for 16 h to reverse the crosslinking. This was followed by the addition of 10 μg of RNase/ml and the DNA was purified by phenol–chloroform extraction. Then, 300 ng of DNA was analyzed by quantitative real-time PCR, performed with SYBR GreenER qPCR Mastermix (Invitrogen) using primers listed in Table 1. Cycling was performed on a Applied Biosystems Prism 7900HT Sequence Detection System (Applied Biosystems, Foster City, CA) with the following parameters: 50 °C for 2 min, *Taq* activation at 95 °C for 10 min, then 40 cycles of 95 °C for 15 s and 60 °C for 1 min. Reactions were performed in triplicate and specificity monitored using melting curve analysis after cycling. Crosslinking efficiency was calculated as described previously.[33]

Chromatin immunoprecipitation

In vivo ChIP assay was performed by using ChIP-IT Express kit (Active Motif, Carlsbad, CA) according to the manufacturer's protocol. Briefly, kidneys from hHO-1 BAC transgenic mice were collected and sliced into small pieces (1–3 mm^3) using a razor blade or scalpel. Then, tissues were transferred into 15 ml conical tubes containing 10 ml fixation solution (1% formaldehyde in minimal cell culture medium). Cells were resuspended completely and rotate tube at room temperature for 10 min. Crosslinking was stopped by adding 1 ml 10 × Glycine Stop-Fix Solution, rotate 5 min at room temperature. Cells were pelleted by centrifuging for 5 min at 720 RCF followed by resuspension in 1.5 ml ice-cold Lysis Buffer. After homogenization, nuclear extract was digested with 3.3 U of Enzymatic Shearing Cocktail for 15 min at 37 °C. The enzyme reaction was stopped by adding EDTA and then the sheared chromatin was collected after centrifugation for 10 min at 4 °C. Then, 2 μg of indicated antibodies as well as IgG control were used for pulling down in 7 μg of sheared chromatin. After 16 h of incubation at 4 °C, magnetic beads were washed and chromatin was eluted by adding Reverse Crosslink Buffer. Quantitative real-time PCR was used for analysis as described earlier.[33]

Rhabdomyolysis

Glycerol model of rhabdomyolysis was induced in age-matched hHO-1 BAC, HO-1$^{+/+}$, and HO-1$^{-/-}$ mice deprived of water for 16 h as described previously.[62] Mice were anesthetized by isoflurane and were injected with 50% glycerol in water or saline as a control, 7.5 ml/kg body weight, with half the volume delivered into each anterior thigh muscle. Mice were killed 3 h after injection for the ChIP and 3C assay and at 4 and 8 h for HO-1 mRNA and at 16 h for HO-1 protein and enzyme activity measurements. Survival studies were performed in additional hHO-1 BAC, HO-1$^{+/+}$, and HO-1$^{-/-}$ mice ($n = 10$/group).

Cisplatin injury model

HO-1$^{+/+}$ and hHO-1 BAC mice (8 to 14 weeks of age) were administered 20 mg/kg body weight cisplatin (1.0 mg/ml solution in sterile 0.9% NaCl) or normal saline by a single intraperitoneal injection. All animals were killed at the indicated time points after cisplatin administration and kidneys were harvested for HO-1 mRNA and protein and enzyme activity measurements. Blood was collected via heart puncture and serum was isolated for creatinine determination.

Statistical analysis

All the experiments were performed at least three times. Results are expressed as mean ± s.e.m. and are derived from three independent experiments. Student's *t*-test and analysis of variance with Student-Newman-Keuls post-test was used for comparisons. All results are considered significant at $P < 0.05$.

DISCLOSURE

All the authors declared no competing interests.

ACKNOWLEDGMENTS

This work was supported by the NIH grants R01 DK59600 and R01 DK75532, the core resource of the UAB-UCSD O'Brien Center (P30 DK079337; to AA), and the AHA grant 0655318B (to JFG). We greatly appreciate the assistance of Dr Robert Kesterson (UAB Transgenic Mouse Facility), Dr Sumant Chugh, and Dr. Daniel Sharer (Bioanalytical Core of the O'Brien Center). We acknowledge the technical assistance of Reny Joseph and Daniel McFalls.

SUPPLEMENTARY MATERIAL

Figure 1. HO-1 and HO-2 protein expression in HO-1 BAC and hHO-1 BAC mice.
Figure 2. HO-1 mRNA, protein and enzyme activity in hHO-1 BAC mice following cisplatin administration.
Figure 3. Overexpression of USF1 and USF2 induces endogenous HO-1 expression in HEK293 cells.
Figure 4. USF1 and Sp1 are involved in chromatin looping during the HO-1 transcription.
Figure 5. CTCF binds to multiple regulatory regions of the human HO-1.
Supplementary material is linked to the online version of the paper at http://www.nature.com/ki

REFERENCES

1. Tenhunen R, Marver HS, Schmid R. Microsomal heme oxygenase. Characterization of the enzyme. *J Biol Chem* 1969; **244**: 6388–6394.
2. Maines MD. The heme oxygenase system: a regulator of second messenger gases. *Annu Rev Pharmacol Toxicol* 1997; **37**: 517–554.
3. Yoshida T, Kikuchi G. Purification and properties of heme oxygenase from pig spleen microsomes. *J Biol Chem* 1978; **253**: 4224–4229.
4. Hayashi S, Omata Y, Sakamoto H *et al.* Characterization of rat heme oxygenase-3 gene. Implication of processed pseudogenes derived from heme oxygenase-2 gene. *Gene* 2004; **336**: 241–250.
5. Poss KD, Tonegawa S. Heme oxygenase 1 is required for mammalian iron reutilization. *Proc Natl Acad Sci USA* 1997; **94**: 10919–10924.
6. Otterbein LE, Soares MP, Yamashita K *et al.* Heme oxygenase-1: unleashing the protective properties of heme. *Trends Immunol* 2003; **24**: 449–455.
7. Nath KA. Heme oxygenase-1: a provenance for cytoprotective pathways in the kidney and other tissues. *Kidney Int* 2006; **70**: 432–443.
8. Maines MD, Mayer RD, Ewing JF *et al.* Induction of kidney heme oxygenase-1 (HSP32) mRNA and protein by ischemia/reperfusion: possible role of heme as both promotor of tissue damage and regulator of HSP32. *J Pharmacol Exp Ther* 1993; **264**: 457–462.
9. Shimizu H, Takahashi T, Suzuki T *et al.* Protective effect of heme oxygenase induction in ischemic acute renal failure. *Crit Care Med* 2000; **28**: 809–817.

10. Mosley K, Wembridge DE, Cattell V *et al.* Heme oxygenase is induced in nephrotoxic nephritis and hemin a stimulator of heme oxygenase synthesis, ameliorates disease. *Kidney Int* 1998; **53**: 672–678.
11. Nath KA, Grande JP, Haggard JJ *et al.* Oxidative stress and induction of heme oxygenase-1 in the kidney in sickle cell disease. *Am J Pathol* 2001; **158**: 893–903.
12. Agarwal A, Balla J, Alam J *et al.* Induction of heme oxygenase in toxic renal injury: a protective role in cisplatin nephrotoxicity in the rat. *Kidney Int* 1995; **48**: 1298–1307.
13. Agarwal A, Kim Y, Matas AJ *et al.* Gas-generating systems in acute renal allograft rejection in the rat. Co-induction of heme oxygenase and nitric oxide synthase. *Transplantation* 1996; **61**: 93–98.
14. Avihingsanon Y, Ma N, Csizmadia E *et al.* Expression of protective genes in human renal allografts: a regulatory response to injury associated with graft rejection. *Transplantation* 2002; **73**: 1079–1085.
15. Tullius SG, Nieminen-Kelha M, Buelow R *et al.* Inhibition of ischemia/reperfusion injury and chronic graft deterioration by a single-donor treatment with cobalt-protoporphyrin for the induction of heme oxygenase-1. *Transplantation* 2002; **74**: 591–598.
16. Nath KA, Balla G, Vercellotti GM *et al.* Induction of heme oxygenase is a rapid, protective response in rhabdomyolysis in the rat. *J Clin Invest* 1992; **90**: 267–270.
17. Nath KA, Haggard JJ, Croatt AJ *et al.* The indispensability of heme oxygenase-1 in protecting against acute heme protein-induced toxicity in vivo. *Am J Pathol* 2000; **156**: 1527–1535.
18. Poss KD, Tonegawa S. Reduced stress defense in heme oxygenase 1-deficient cells. *Proc Natl Acad Sci USA* 1997; **94**: 10925–10930.
19. Imai T, Morita T, Shindo T *et al.* Vascular smooth muscle cell-directed overexpression of heme oxygenase-1 elevates blood pressure through attenuation of nitric oxide-induced vasodilation in mice. *Circ Res* 2001; **89**: 55–62.
20. Maines MD, Polevoda B, Coban T *et al.* Neuronal overexpression of heme oxygenase-1 correlates with an attenuated exploratory behavior and causes an increase in neuronal NADPH diaphorase staining. *J Neurochem* 1998; **70**: 2057–2069.
21. Duann P, Lianos EA. GEC-targeted HO-1 expression reduces proteinuria in glomerular immune injury. *Am J Physiol Renal Physiol* 2009; **297**: F629–F638.
22. Yet SF, Tian R, Layne MD *et al.* Cardiac-specific expression of heme oxygenase-1 protects against ischemia and reperfusion injury in transgenic mice. *Circ Res* 2001; **89**: 168–173.
23. Sabaawy HE, Zhang F, Nguyen X *et al.* Human heme oxygenase-1 gene transfer lowers blood pressure and promotes growth in spontaneously hypertensive rats. *Hypertension* 2001; **38**: 210–215.
24. Tu CF, Kuo CH, Juang JH. Effects of heme oxygenase-1 transgenic islets on transplantation. *Transplant Proc* 2005; **37**: 3463–3467.
25. Braudeau C, Bouchet D, Toquet C *et al.* Generation of heme oxygenase-1-transgenic rats. *Exp Biol Med (Maywood)* 2003; **228**: 466–471.
26. Melo LG, Agrawal R, Zhang L *et al.* Gene therapy strategy for long-term myocardial protection using adeno-associated virus-mediated delivery of heme oxygenase gene. *Circulation* 2002; **105**: 602–607.
27. Sikorski EM, Hock T, Hill-Kapturczak N *et al.* The story so far: molecular regulation of the heme oxygenase-1 gene in renal injury. *Am J Physiol Renal Physiol* 2004; **286**: F425–F441.
28. Kitamuro T, Takahashi K, Ogawa K *et al.* Bach1 functions as a hypoxia-inducible repressor for the heme oxygenase-1 gene in human cells. *J Biol Chem* 2003; **278**: 9125–9133.
29. Sikorski EM, Uo T, Morrison RS *et al.* Pescadillo interacts with the cadmium response element of the human heme oxygenase-1 promoter in renal epithelial cells. *J Biol Chem* 2006; **281**: 24423–24430.
30. Alam J, Wicks C, Stewart D *et al.* Mechanism of heme oxygenase-1 gene activation by cadmium in MCF-7 mammary epithelial cells. Role of p38 kinase and Nrf2 transcription factor. *J Biol Chem* 2000; **275**: 27694–27702.
31. Lee PJ, Jiang BH, Chin BY *et al.* Hypoxia-inducible factor-1 mediates transcriptional activation of the heme oxygenase-1 gene in response to hypoxia. *J Biol Chem* 1997; **272**: 5375–5381.
32. Shibahara S, Nakayama M, Kitamuro T *et al.* Repression of heme oxygenase-1 expression as a defense strategy in humans. *Exp Biol Med (Maywood)* 2003; **228**: 472–473.
33. Deshane J, Kim J, Bolisetty S *et al.* Sp1 regulates chromatin looping between an intronic enhancer and distal promoter of the human heme oxygenase-1 gene in renal cells. *J Biol Chem* 2010; **285**: 16476–16486.
34. Hill-Kapturczak N, Sikorski E, Voakes C *et al.* An internal enhancer regulates heme-and cadmium-mediated induction of human heme oxygenase-1. *Am J Physiol Renal Physiol* 2003; **285**: F515–F523.
35. Hock TD, Liby K, Wright MM *et al.* JunB and JunD regulate human heme oxygenase-1 gene expression in renal epithelial cells. *J Biol Chem* 2007; **282**: 6875–6886.
36. Hock TD, Nick HS, Agarwal A. Upstream stimulatory factors USF1 and USF2, bind to the human haem oxygenase-1 proximal promoter in vivo and regulate its transcription. *Biochem J* 2004; **383**: 209–218.
37. Kapturczak MH, Wasserfall C, Brusko T *et al.* Heme oxygenase-1 modulates early inflammatory responses: evidence from the heme oxygenase-1-deficient mouse. *Am J Pathol* 2004; **165**: 1045–1053.
38. Park DJ, Agarwal A, George JF. Heme oxygenase-1 expression in murine dendritic cell subpopulations: effect on CD8+ dendritic cell differentiation in vivo. *Am J Pathol* 2010; **176**: 2831–2839.
39. Chernukhin I, Shamsuddin S, Kang SY *et al.* CTCF interacts with and recruits the largest subunit of RNA polymerase II to CTCF target sites genome-wide. *Mol Cell Biol* 2007; **27**: 1631–1648.
40. Ohlsson R, Lobanenkov V, Klenova E. Does CTCF mediate between nuclear organization and gene expression? *Bioessays* 2010; **32**: 37–50.
41. Phillips JE, Corces VG. CTCF: master weaver of the genome. *Cell* 2009; **137**: 1194–1211.
42. Splinter E, Heath H, Kooren J *et al.* CTCF mediates long-range chromatin looping and local histone modification in the beta-globin locus. *Genes Dev* 2006; **20**: 2349–2354.
43. Ohlsson R, Renkawitz R, Lobanenkov V. CTCF is a uniquely versatile transcription regulator linked to epigenetics and disease. *Trends Genet* 2001; **17**: 520–527.
44. Filippova GN. Genetics and epigenetics of the multifunctional protein CTCF. *Curr Top Dev Biol* 2008; **80**: 337–360.
45. Hou C, Dale R, Dean A. Cell type specificity of chromatin organization mediated by CTCF and cohesin. *Proc Natl Acad Sci USA* 2010; **107**: 3651–3656.
46. Cai S, Lee CC, Kohwi-Shigematsu T. SATB1 packages densely looped, transcriptionally active chromatin for coordinated expression of cytokine genes. *Nat Genet* 2006; **38**: 1278–1288.
47. Horike S, Cai S, Miyano M *et al.* Loss of silent-chromatin looping and impaired imprinting of DLX5 in Rett syndrome. *Nat Genet* 2005; **37**: 31–40.
48. Kumar PP, Bischof O, Purbey PK *et al.* Functional interaction between PML and SATB1 regulates chromatin-loop architecture and transcription of the MHC class I locus. *Nat Cell Biol* 2007; **9**: 45–56.
49. Otterbein LE, Choi AM. Heme oxygenase: colors of defense against cellular stress. *Am J Physiol Lung Cell Mol Physiol* 2000; **279**: L1029–L1037.
50. Abraham NG, Kappas A. Heme oxygenase and the cardiovascular-renal system. *Free Radic Biol Med* 2005; **39**: 1–25.
51. Brouard S, Otterbein LE, Anrather J *et al.* Carbon monoxide generated by heme oxygenase 1 suppresses endothelial cell apoptosis. *J Exp Med* 2000; **192**: 1015–1026.
52. Agarwal A, Nick HS. Renal response to tissue injury: lessons from heme oxygenase-1 gene ablation and expression. *J Am Soc Nephrol* 2000; **11**: 965–973.
53. Abshagen K, Eipel C, Kalff JC *et al.* Kupffer cells are mandatory for adequate liver regeneration by mediating hyperperfusion via modulation of vasoactive proteins. *Microcirculation* 2008; **15**: 37–47.
54. Bauer I, Wanner GA, Rensing H *et al.* Expression pattern of heme oxygenase isoenzymes 1 and 2 in normal and stress-exposed rat liver. *Hepatology* 1998; **27**: 829–838.
55. Guo G, Bhat NR. Hypoxia/reoxygenation differentially modulates NF-kappaB activation and iNOS expression in astrocytes and microglia. *Antioxid Redox Signal* 2006; **8**: 911–918.
56. Vallian S, Chin KV, Chang KS. The promyelocytic leukemia protein interacts with Sp1 and inhibits its transactivation of the epidermal growth factor receptor promoter. *Mol Cell Biol* 1998; **18**: 7147–7156.
57. Kie JH, Kapturczak MH, Traylor A *et al.* Heme oxygenase-1 deficiency promotes epithelial-mesenchymal transition and renal fibrosis. *J Am Soc Nephrol* 2008; **19**: 1681–1691.
58. Strober W. Wright-Giemsa and nonspecific esterase staining of cells. *Curr Protoc Immunol* 2001 Appendix 3: Appendix 3C.
59. Ferguson DJ, Lee SF, Gordon PA. Evaluation of reticulocyte counts by flow cytometry in a routine laboratory. *Am J Hematol* 1990; **33**: 13–17.
60. Dekker J, Rippe K, Dekker M *et al.* Capturing chromosome conformation. *Science* 2002; **295**: 1306–1311.
61. Tolhuis B, Palstra RJ, Splinter E *et al.* Looping and interaction between hypersensitive sites in the active beta-globin locus. *Mol Cell* 2002; **10**: 1453–1465.
62. Dorman RB, Wunder C, Brock RW. Cobalt protoporphyrin protects against hepatic parenchymal injury and microvascular dysfunction during experimental rhabdomyolysis. *Shock* 2005; **23**: 275–280.